ESTIMATION OF NEAR FIELD CHARACTERISTICS OF EARTHQUAKE MOTION

by

Don Tocher[I], Ashok S. Patwardhan[II], and Lloyd S. Cluff[III]

SYNOPSIS

Estimation of strong earthquake ground motion in the near field is a complex problem because, in addition to the earthquake magnitude and distance, source characteristics and geometry and the characteristics of transmission path significantly influence the attenuation of ground motion. Available strong motion data in the near field are scanty and frequently need reevaluation. Because uncertainties are associated at present with the actual values and physical relationships governing source characteristics, a probabilistic approach offers considerable advantage for a systematic evaluation of data. The importance of re-evaluation of geologic and seismologic data for engineering purposes is illustrated by two examples.

INTRODUCTION

Current seismic design procedures utilize peak acceleration (a_p) as one of the parameters for defining design earthquakes. This acceleration is usually established by using an empirical magnitude-acceleration-distance relationship implying a point source model (see Figure 1). In the near field (i.e., when the dimensions of the rupture surface and the distances to the location of interest are of the same order of magnitude), it is not realistic to model the earthquake as an event of a given magnitude releasing energy at an instrumentally determined focus. Rather, additional factors need to be taken into account, such as ambient stress, stress drop, material properties at the fault surface and in the radiation path, size of rupture surface, and source mechanism. The effect of these factors can be significant. Very limited data are available for verifying the validity of the attenuation relationships in the near field, and those that are available show wide scatter. Especially, strong motion recordings from some recent earthquakes have shown high accelerations and anomalous attenuation characteristics in the near field [for example, a_p = 1.5 g, Pacoima Dam, San Fernando earthquake, February 9, 1971 (M6.6); a_p = 0.69 g, Stone Canyon earthquake, September 4, 1972 (M4.7); a_p = 0.40 g, Ancona, Italy, June 14, 1972 (M4.9); a_p = 0.63 g, Koyna, India, December 10, 1967 (M6.5)].

To improve the accuracy of estimated peak accelerations, a two-step procedure appears most appropriate: (a) take into account some of the

---

I Chief Seismologist, Woodward-Clyde Consultants, San Francisco, CA, USA.

II Senior Project Engineer, Woodward-Clyde Consultants, San Francisco, CA, USA.

III Principal Engineering Geologist, Woodward-Clyde Consultants, San Francisco, CA, USA.

above-named factors in a more comprehensive manner, and (b) reevaluate available data to examine reasons for apparent anomalies. This paper presents an approach to both steps (a) and (b).

(a) Considerations of Source Conditions: In the approach illustrated in Figure 2, the maximum acceleration at a location very close to the fault is first established based on source conditions. Next, the likely attenuation path is established to a suitable distance. Thus, the procedure is opposite to the customary one.

Because several uncertainties are involved in both the magnitude and physical relationships governing the factors, a probabilistic approach is most advantageous at present for estimating the likelihood of a given acceleration being exceeded at a given point. Because the frequency content and the geometry of the radiation field are dependent, to some extent, upon the size of the rupture zone (i.e., earthquake magnitude), the term "near field" should realistically connote a distance increasing, within limits, with magnitude. In concept, this distance will be a multiple of the rupture length for small to moderate earthquakes within which peak accelerations are associated with high frequency waves ($f \simeq 25$ Hz). Based on estimates of size of rupture surfaces, this distance may be 0 to 20 km with a probable upper limit of 30 km for larger earthquakes. Several relationships between source parameters have been proposed; the most useful ones are:

$$M_o = \mu A \bar{D} \quad ; \quad \ddot{u} = \frac{2\sigma}{\rho\beta\Delta t} \qquad (1)$$

where: $\Delta t \simeq f$; $\ddot{u} = \infty$ if $\Delta t \to 0$

$$\ddot{u} = \frac{\tilde{\sigma}}{\rho R} \qquad (2)$$

$$\log M_o = 1.5 \log A + \log \Delta\sigma + \log C \; ; \; M_s \sim \log L^2 \text{(small earthquakes)} \; ;$$

$$M_s \sim \log L^3 \text{ (moderate to large earthquakes)} \; ; \; \frac{W}{L} = \text{const}(C_1) \; ;$$

$$\frac{\bar{D}}{L} = \text{const}(C_2) \; ; \; \frac{v\tau}{L} = \text{const}(C_3) \qquad (3) \, .$$

where: M_o = seismic moment, $\bar{u}$ = average displacement, σ = effective dynamic stress, $\Delta\sigma$ = stress drop, $\tilde{\sigma}$ = tectonic stress, L = rupture length, W = rupture width, v = velocity, τ = rupture duration, M_s = surface wave magnitude.

Using the above equations and assuming $\sigma \simeq \Delta\sigma$, the maximum acceleration very close to a rupture surface of length L is given by:

$$\ddot{u} = \frac{2Cn\mu}{\rho\beta\Delta t} \left(\frac{\bar{D}}{L}\right)$$

If the values of β and μ are known and $\bar{D}$ can be estimated, the value of $\ddot{u}$ may be determined. However, in the absence of reliable data, probabilistic relationships may be established to account for variations in the parameters (see Figure 2).

The next step consists of establishing the slope of the attenuation curve (i.e., line AB in Figure 2). To define the shape of the attenuation

relationship in the near field, the concept of significant distance is introduced. Significant distance is an appropriate distance from the rupture surface to the point in question. Examples of evaluation of significant distance are given in the next section. In general, the attenuation of peak acceleration may be represented by:

$$\log a_{px} = x \log a_{po} + C$$

Based on the above equations, we may write for the probability of experiencing a peak acceleration a_{px}.

$$P[a_{px}] = \sum_{\text{source } 1}^{n} P(a_{px}|\Delta\sigma,\bar{D})\ P(\Delta\sigma,\bar{D}) + P(a_{px}|M_s)\ P(M_s) + P(a_{px}|\gamma)\ P(\gamma)$$

Schematic distributions for each of the above variables are sketched in Figure 2.

(b) Reevaluation of Available Data: Two examples are chosen to illustrate the procedure: the San Fernando earthquake of February 9, 1971 (M6.6) and the Stone Canyon earthquake of September 4, 1972 (M4.7).

San Fernando Earthquake: The earthquake (epicenter 34.40N, 118.39°W, focal depth 13 km) was recorded at 65 stations, three of which [Pacoima Dam, Castaic, and Lake Hughes No. 12 (4)] reported anomalously high accelerations (see Figure 3a). The rupture surface of the earthquake was defined by the aftershocks precisely located by Hanks (5) and others, who also relocated the epicenter an additional 2.5 miles north so that the focal depth would coincide with the rupture surface defined by the precisely determined aftershock zone. Figure 3b is a schematic cross section showing the location of surface rupture, epicenter, and the use of significant distance. The epicentral distances for Pacoima Dam, Lake Hughes, and Castaic are 8, 24, and 27 km, respectively. The corresponding significant distances are distances measured from the accelerograph stations to the rupture surfaces, which are reduced to 3, 18, and 20 km, respectively.

Stone Canyon Earthquake: The Stone Canyon earthquake (epicenter 36.63N, 121.26W, focal depth ≃ 5 km). The earthquake produced some unusual accelerographs at three stations (4): Melendy Ranch, Stone Canyon Observatory, and the Bear Valley fire station (see Figure 4a). Figure 4a is based on a paper by Wesson and Ellsworth (6) using the microearthquake network of the U. S. Geological Survey in this part of California. The zone of aftershocks was located as shown in the upper left area of Figure 4a with the epicenter somewhere in the middle of that zone.

To realistically interpret strong motion data obtained from the three accelerograph stations, geologic conditions in the area and the limitations and accuracy of the epicenter location procedure must be taken into account. Geologic conditions in the area clearly indicate that the epicenter of this earthquake should lie on the well-recognized trace of the San Andreas fault. The fact that it does not is an artifact of the model used in the locating program. Furthermore, the fresh ruptures

seen in the fault zone can be considered to be located within the rupture zone of the main earthquake. As suggested by Wesson and Ellsworth (6), this zone had an extent approximately as long as the aftershock zone shown in Figure 4a. The shape and size of the aftershock zone was extremely well determined by the seismograph stations, even if its location was biased by assumptions of constant wave velocities on either side of the fault. Therefore, the relative locations of the group of events is better than the absolute location of any one of them. The southern end of the aftershock zone can be anchored to the ruptures in the fault zone, as shown in Figure 4b.

Tying this zone to the observed ground rupture produces rather dramatic effects on the strong motion pattern as recorded by the three accelerograph stations and the significant distances. The peak accelerations recorded at Melendy Ranch, Stone Canyon, and Bear Valley were 0.69 g, 0.22 g, and 0.18 g, respectively. The corresponding epicentral distances based on Figure 4a are 8, 1.9, and 9.6 km. Their significant distances based on the distance to rupture surface are 0.15, 1.9, and 1.9 km.

Attenuation Based on Significant Distance: The effect of using significant distances for attenuation of peak acceleration in the near field can be assessed from Figure 5, which shows a comparison of the peak acceleration vs. epicentral distance and peak acceleration vs. significant distance for the 1971 San Fernando earthquake and the 1972 Stone Canyon earthquake. Undoubtedly, in both cases, plotting the data in terms of significant distance provides a better interpretation of the recorded peak accelerations. The stations closest to the rupture surface now have the highest peak acceleration; and the accelerations decrease in an orderly fashion with distance, thereby reducing the scatter in the data that provide the basis for empirical relationships.

SELECTED REFERENCES

(1) Brune, James N., 1970, Tectonic stress and the spectra of seismic shear waves from earthquakes: Journal of Geophysical Research, v. 75, no. 26, p. 4997-5009.

(2) Hanks, Thomas C., and Johnson, Dennis A., 1976, Geophysical assessment of peak accelerations: Bulletin of the Seismological Society of America, in press.

(3) Kanamori, Hiroo, and Anderson, Don L., 1975, Theoretical basis of some empirical relations in seismology: Bulletin of the Seismological Society of America, v. 65, no. 5, p. 1073-1095.

(4) Earthquake Engineering Research Laboratory, California Institute of Technology (EERL-CIT), Strong motion earthquake accelerograms, Vol. II (Corrected accelerograms and integrated ground velocity and displacement curves).

(5) Hanks, T. C., 1974, The faulting mechanics of the San Fernando earthquake: Journal of Geophysical Research, v. 79, no. 8, p. 1215-1229.

(6) Wesson, R. L., and Ellsworth, W. L., 1972, Preliminary hypocentral data for the Stone Canyon earthquake of September 4, 1972: Earthquake Notes, Eastern Section of Geological Society of America, v. XLIII, no. 3.

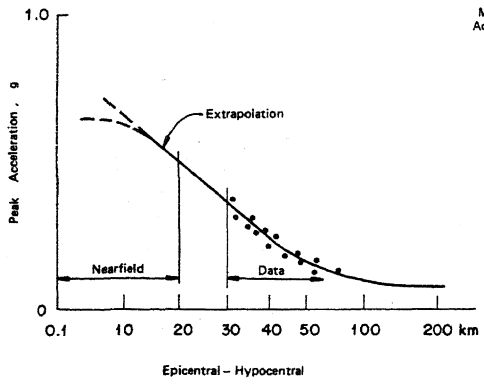

Figure 1. ATTENUATION CURVE

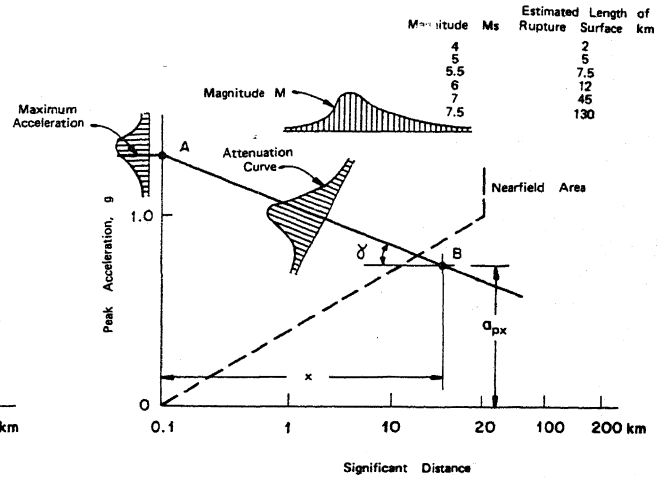

Figure 2. APPROACH TO ESTIMATION OF NEARFIELD ATTENUATION RELATIONSHIP

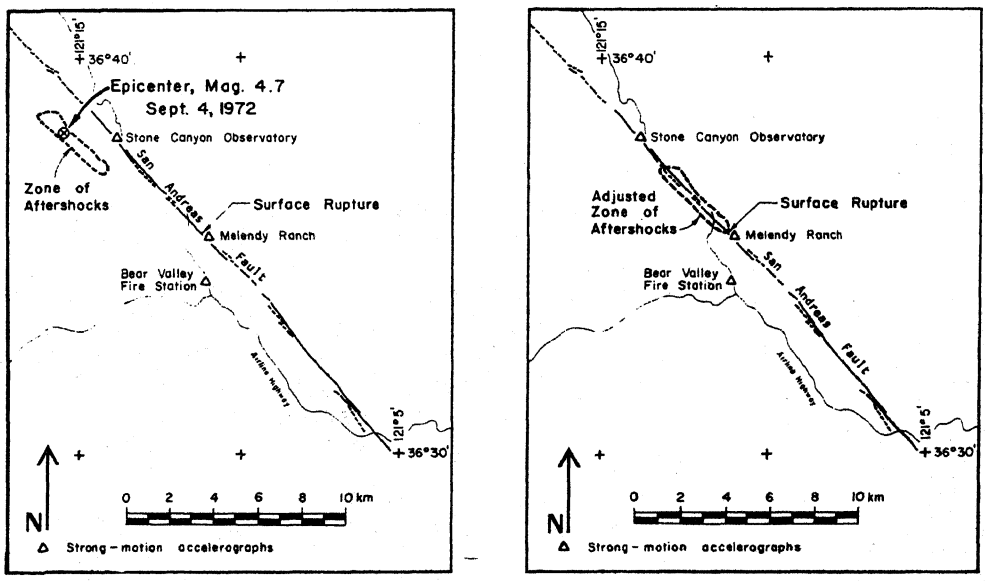

Figure 3. STONE CANYON EARTHQUAKE SEPTEMBER 4, 1972
REEVALUATION OF AFTERSHOCK FOCI AND
SIGNIFICANT DISTANCE

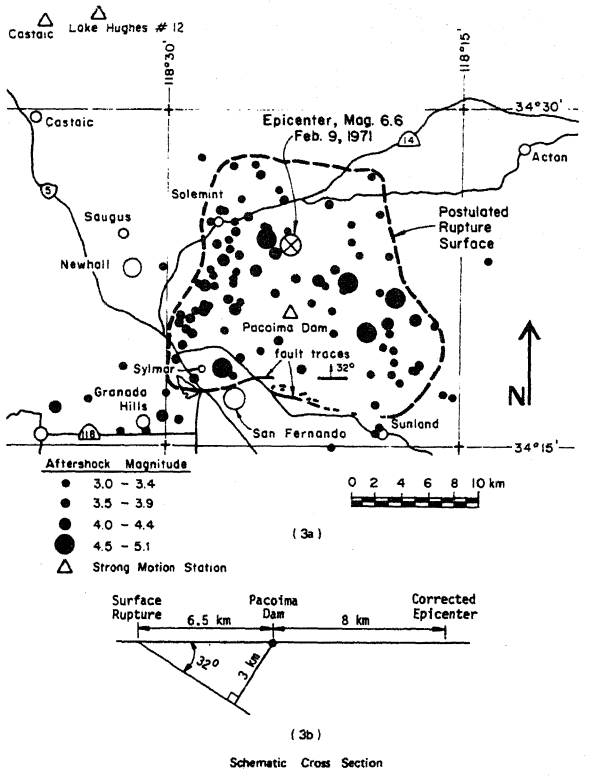

Figure 4. SAN FERNANDO EARTHQUAKE FEBRUARY 9, 1971
EVALUATION OF SIGNIFICANT DISTANCE

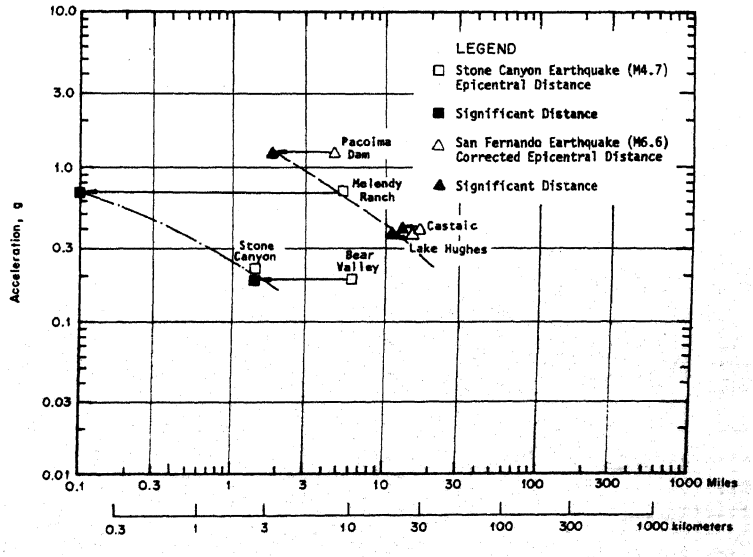

Figure 5. SAN FERNANDO AND STONE CANYON EARTHQUAKE
REEVALUATION OF DATA

DISCUSSION

I.N. Gupta (U.S.A)

Very large earthquakes ($M \geq 7$) may have rupture lengths as large as 100 km or more. How do you distinguish between near-field and far-field epicentral distances in such cases ?

Author's Closure

Not received.